Control Barrier Corridors: From Safety Functions to Safe Goal Sets

Ömür Arslan and Nikolay Atanasov

***Abstract*— Safe autonomy is a critical requirement and a key enabler for robots to operate in complex environments. Control barrier functions and safe motion corridors are two widely used but distinct safety methods, functional and geometric, respectively, for planning and control. Control barrier functions filter control inputs to limit the decay rate of safety, whereas safe motion corridors are geometrically constructed to define a local safe zone around the system state. This paper introduces a new notion of *control barrier corridors*, unifying these two approaches by converting control barrier functions into local safe goal regions for reference goal selection in feedback control systems. We show, with examples on fully actuated systems, kinematic unicycles, and linear output regulation systems, that *individual state safety can be extended locally over control barrier corridors* for convex barrier functions, provided the control convergence rate matches the barrier decay rate. Such safe control barrier corridors enable safely reachable persistent goal selection over continuously changing barrier corridors during motion, which we demonstrate for verifiably safe path following in autonomous exploration of unknown environments.**

I. Introduction

Ensuring that autonomous systems operate safely while achieving performance and stability objectives has emerged as a central challenge in robotics and automation. Control barrier functions (CBFs) [1] have recently gained significant traction as a principled tool for enforcing safety by modifying control inputs to bound the safety decay rate. CBFs have also been combined with control Lyapunov functions (CLFs) [2] to reconcile joint stability and safety requirements [3]. In parallel, geometrically constructed safe motion corridors have been applied for motion planning [4] and combined with reference governor techniques [5], [6] to achieve safety guarantees without interfering with stability [7]. Understanding the connections among CBFs, reference governors, and safe motion corridors has the potential to offer new insights, combine their strengths, and mitigate their limitations [8].

This paper introduces a new unifying approach to transform the functional safety constraints of CBFs into geometric safety restrictions on reference goals for feedback control systems. Specifically, we consider a given stabilizing control law for the system and study the set of goals that satisfy CBF safety constraints. We refer to this region of safe closed-loop system goals as a *control barrier corridor*. Our key insight is that individual state safety imposed through CBFs can be extended locally into a control barrier corridor, under appropriate conditions on the barrier functions, their decay profiles, and the closed-loop system convergence rate. In particular, we show that, if (i) the barrier functions are convex and (ii) the barrier decay rate matches the closed-loop system convergence rate, then simultaneously safely reachable and stable reference goals can be selected from control barrier corridors. This enables verifiably safe and persistent path following of robots by continuously chasing a path goal within their control barrier corridors, as illustrated in Fig. 1.

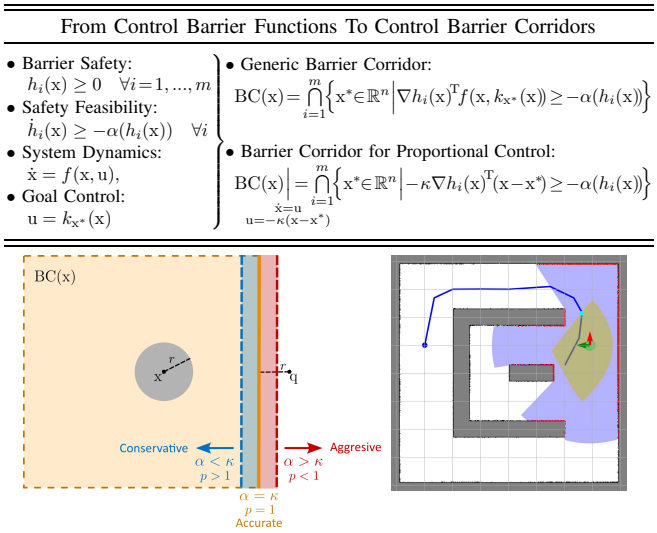

Fig. 1. Control barrier corridors turn CBF safety specification on control inputs into a geometric representation of safe goals for state feedback control. For instance, a control barrier corridor $\mathrm{BC}(\mathrm{x})$ around a safe state x of a fully actuated system $\dot{\mathrm{x}} = \mathrm{u}$ under proportional control $\mathrm{u} = -\kappa(\mathrm{x} - \mathrm{x}^*)$ is the set of goal states x^* that ensure safe control based on the feasibility condition $\dot{h}_i(\mathrm{x}) \geq -\alpha(h_i(\mathrm{x}))$ for a set of CBFs $h_1(\mathrm{x}), \ldots, h_m(\mathrm{x})$. (left) The control barrier corridor of a fully actuated circular robot, centered at x with radius $r > 0$, relative to a point obstacle at q, constructed based on the power-distance barrier function $h(\mathrm{x}) = \|\mathrm{x} - \mathrm{q}\|^p - r^p$. The control barrier corridor enlarges with an increasing ratio of the barrier decay rate to the proportional control gain, $\frac{\alpha}{\kappa}$, and shrinks with the increasing order p of the power distance. (right) The control barrier corridor (yellow) of a fully actuated circular robot (cyan+red arrow), constructed relative to multiple sensed obstacle points (red), captures a local collision-free space around the robot for convex barrier functions (e.g., the power distance with $p \geq 1$) under identical linear barrier decay rate and proportional control gain, $\alpha = \kappa$. This allows for selecting a safely reachable goal (cyan) for following a reference path (blue).

A. Motivation and Related Literature

a) Control Barrier Functions: Safety filtering of control inputs using CBF constraints has become a de facto tool for enforcing safety for complex control systems. A particularly attractive property is that, for any control-affine system, the CBF constraints are linear in the control input, which enables real-time safe control synthesis via convex quadratic optimization [1]. While CBF techniques are elegant and efficient, they modify the control inputs directly and, thus, interfere with the stability properties of the closed-loop

Ömür Arslan is with the Department of Mechanical Engineering, Eindhoven University of Technology, P.O. Box 513, 5600 MB Eindhoven, The Netherlands. Email: o.arslan@tue.nl

Nikolay Atanasov is with the Department of Electrical and Computer Engineering, University of California San Diego, La Jolla, CA 92093, USA. Email: natanasov@ucsd.edu

system. It has been shown that the common strategy of imposing both CBF and CLF constraints and relaxing the stability constraints if safety is endangered leads to undesirable equilibria [9]–[11]. Avoiding this requires the satisfaction of compatibility conditions [12], [13] and potentially modifying the CBF or CLF constraints for compatibility [14], [15]. The performance and conservatism of CBF-based safety filtering also depend on the selection of the barrier decay profiles, and the online adaptation of barrier decay rates can mitigate conservatism [16], [17]. Our analysis offers new insights into the compatibility of safety and stability and the selection of the barrier decay rate relative to the control convergence rate.

b) Reference Governors: Safety filtering of reference goals for pre-stabilized feedback control systems via reference governors [6] is attractive because it ensures safety without interfering with stability. Explicit reference governors can achieve real-time performance comparable to CBF-based safety filters [18]. The key idea of reference governors is that rather than altering the feedback law itself, a governor system is used to filter the desired reference so that the pre-stabilized closed-loop system remains within a safe set. This is achieved by determining invariant sets (e.g., Lyapunov level sets [18] and maximal output admissible sets [19]) to determine how quickly the reference can evolve while ensuring future trajectories remain safe. Local collision-free zones, constructed as safe motion corridors, are also utilized by designing stabilizing feedback laws that also ensure safe zone invariance [20]. Reference governors have been demonstrated in safe trajectory tracking control for integrator [21], linear [22]–[24], unicycle [25], [26], and more complex systems, such as aerial vehicles or manipulators [27], [28].

c) Safe Motion Corridors: Geometrically constructed safe motion corridors are also employed as planning and control constraints for safe, smooth, and dynamically feasible planning [4], [5], as well as for reactive control via reference governors [20]. Such safe corridors are often constructed as a local collision-free geometric zones around obstacles in various convex shapes, including polytopes [5], [29] and boxes [4], [30], by maximizing their volumes to approximately cover the free space around a robot. Safe motion corridors constructed using generalized Voronoi diagrams are applied for safety encoding and safe coordination control of multi-robot systems [31], [32]. In fact, safe corridors constructed based on separating hyperplanes of convex shapes (e.g., spheres) [31], [32] are a special case of control barrier corridors for fully actuated systems, where the barrier functions are given by the Euclidean distance to obstacles, with the proportional control gain matched to the barrier decay rate (as in Proposition 1). We design control barrier corridors to provide a unified functionally generated extension of geometrically constructed safe motion corridors by employing alternative barrier functions for complex control systems [33].

B. Contributions and Organization of the Paper

This paper introduces a new notion of control barrier corridors that systematically convert the functional safety requirements of control barrier functions into local geometric goal zones for safe reference selection in feedback control systems, blending the geometry and dynamics of safety. In summary, the three major contributions of our paper are:

- We propose a generic construction of control barrier corridors for feedback control systems using control barrier functions, as the collection of all goal states around a safe state that ensure barrier safety under feedback control.
- We show that control barrier corridors of fully actuated systems under proportional control encode not only system safety but also goal safety when the barrier functions are convex and the control gain matches the barrier decay rate. We also discuss how this extends to unicycle and linear systems.
- We apply control barrier corridors to select safely reachable goals for sensor-based safe and persistent path following control of a mobile robot in unknown environments.

The rest of the paper is organized as follows. Section II describes how to convert control barrier functions into control barrier corridors. Section III presents example constructions of control barrier corridors and discusses their key properties. Section IV demonstrates an application of control barrier corridors for local goal selection in safe and persistent path following. Section V concludes with a summary of our work and key results and outlines directions for future research.

II. From Barrier Functions to Barrier Corridors

In this section, we review CBFs for safety-critical control systems [1] and present the construction of control barrier corridors for goal-parametrized feedback control systems.

A. Control Barrier Functions

Consider a nonlinear control system with state $\mathrm{x} \in \mathbb{R}^{n_\mathrm{x}}$ and control input $\mathrm{u} \in \mathbb{R}^{n_\mathrm{u}}$ and dynamics specified by a Lipschitz continuous function $f : \mathbb{R}^{n_\mathrm{x}} \times \mathbb{R}^{n_\mathrm{u}} \to \mathbb{R}^{n_\mathrm{x}}$:

$$\dot{\mathrm{x}} = f(\mathrm{x}, \mathrm{u}). \tag{1}$$

Let $\mathcal{X} \subseteq \mathbb{R}^{n_\mathrm{x}}$ denote a set of *safe* system states. A CBF provides sufficient conditions [1] to ensure that $\mathcal{X}$ is forward invariant for the system in (1) by limiting the decay rate of a barrier function whose level set encodes $\mathcal{X}$.

Definition 1 *(Control Barrier Functions)* A continuously differentiable function $h : \mathbb{R}^{n_\mathrm{x}} \to \mathbb{R}$ is a *control barrier function* for the system $\dot{\mathrm{x}} = f(\mathrm{x}, \mathrm{u})$ if

- (*Safe*) $h(\mathrm{x}) \geq 0$ for all $\mathrm{x} \in \mathcal{X}$ and negative otherwise.
- (*Nonsingular*) $\nabla h(\mathrm{x}) \neq 0$ when $h(\mathrm{x}) = 0$.
- (*Feasible*) For any safe state $\mathrm{x} \in \mathcal{X}$ (i.e., $h(\mathrm{x}) \geq 0$), there exist some control input $\mathrm{u} \in \mathbb{R}^{n_\mathrm{u}}$ such that

$$\dot{h}(\mathrm{x}) = \nabla h(\mathrm{x})^{\mathrm{T}} f(\mathrm{x}, \mathrm{u}) \geq -\alpha(h(\mathrm{x}))$$

where $\alpha : \mathbb{R} \to \mathbb{R}$ is a strictly increasing continuous function with $\alpha(0) = 0$ (i.e., a class $\mathcal{K}_\infty$ function).

Intuitively, the nonnegativity of $h(\mathrm{x})$ implicitly specifies the set membership of safe system states in $\mathcal{X}$; the nonsingularity of $\nabla h(\mathrm{x})$ at the safety boundary, where $h(\mathrm{x}) = 0$, is required to clearly indicate the direction of increasing safety; and finally, the feasibility of $h(\mathrm{x})$ ensures that the system can remain safe under some control input, even with a potentially bounded decrease in safety.

Finding a single CBF to encode safety for complex systems (e.g., mobile robot moving in cluttered environment) is a known challenge. Alternatively, multiple simple barrier functions, say $h_1(\mathrm{x}), \ldots, h_m(\mathrm{x})$, can be used simultaneously. In either case, the CBFs can be imposed as safety constraints [34] to minimally modify a desired control policy $\mathrm{u}_d(\mathrm{x})$ for the system in (1), serving as a safety filtering as follows:

$$\begin{aligned} &\underset{\mathrm{u}\in\mathbb{R}^{n_\mathrm{u}}}{\text{minimize}} \;\; \|\mathrm{u}-\mathrm{u}_d(\mathrm{x})\|^2 \\ &\text{subject to} \;\; \nabla h_i(\mathrm{x})^{\mathrm{T}} f(\mathrm{x},\mathrm{u}) \geq -\alpha(h_i(\mathrm{x})) \;\; \forall i=1,\ldots,m. \end{aligned} \tag{2}$$

Safety filtering is often applied to control-affine systems, $\dot{\mathrm{x}} = f(\mathrm{x}) + g(\mathrm{x})\mathrm{u}$, in which case the CBF constraints become affine in the control input and the safety filtering problem becomes a convex quadratic optimization.

In this paper, we show that convexity of the CBFs themselves is also a critical feature for relating and extending the functional safety of individual states to a local geometric safety zone around the safe state. To demonstrate this, we consider the p^{th}-order power distance as a safety measure for a robot with respect to an obstacle point q:

$$h_{\mathrm{pwr}}(\mathrm{x}) := \|\mathrm{x}-\mathrm{q}\|^p - r^p, \tag{3}$$

where $r > 0$ represents a safety margin, e.g., the robot or obstacle radius. The gradient and Hessian of $h_{\mathrm{pwr}}(\mathrm{x})$ are:

$$\nabla h_{\mathrm{pwr}}(\mathrm{x}) = p\|\mathrm{x}-\mathrm{q}\|^{p-2}(\mathrm{x}-\mathrm{q}), \tag{4}$$

$$\nabla^2 h_{\mathrm{pwr}}(\mathrm{x}) = p\|\mathrm{x}-\mathrm{q}\|^{p-2}\Big(\mathbf{I} + (p-2)\tfrac{(\mathrm{x}-\mathrm{q})(\mathrm{x}-\mathrm{q})^{\mathrm{T}}}{\|\mathrm{x}-\mathrm{q}\|^2}\Big). \tag{5}$$

Note that the power distance $h_{\mathrm{pwr}}(\mathrm{x})$ is convex for $p \geq 1$.

B. Control Barrier Corridors

CBFs are primarily utilized to determine the safety of individual states and the associated control constraints but their connection to local safety around a given state remains unexplored. To extend the safety of an individual state to a local safety zone, we consider a given goal-parametrized state-feedback control policy (or goal control, for short) $\mathrm{u} = k_{\mathrm{x}^*}(\mathrm{x})$ that can bring the system $\dot{\mathrm{x}} = f(\mathrm{x},\mathrm{u})$ to a goal state $\mathrm{x}^* \in \mathbb{R}^{n_\mathrm{x}}$. We define the *control barrier corridor* associated with a set of CBFs and a goal control policy as the set of all goal states that induce safe feedback control.

Definition 2 (*Control Barrier Corridor*) The *control barrier corridor* of a system $\dot{\mathrm{x}} = f(\mathrm{x},\mathrm{u})$ with goal-control policy $\mathrm{u} = k_{\mathrm{x}^*}(\mathrm{x})$ and a set of CBFs $h_1(\mathrm{x}), \ldots, h_m(\mathrm{x})$, denoted by $\mathrm{BC}(\mathrm{x})$, around a safe state $\mathrm{x} \in \mathbb{R}^{n_\mathrm{x}}$ (with $h_i(\mathrm{x}) \geq 0$ for all i) is defined as the set of all goal states $\mathrm{x}^* \in \mathbb{R}^{n_\mathrm{x}}$ that result in a safe control input under the goal control $\mathrm{u} = k_{\mathrm{x}^*}(\mathrm{x})$:

$$\mathrm{BC}(\mathrm{x}) := \bigcap_{i=1}^{m} \Big\{ \mathrm{x}^* \in \mathbb{R}^{n_\mathrm{x}} \Big| \nabla h_i(\mathrm{x})^{\mathrm{T}} f(\mathrm{x}, k_{\mathrm{x}^*}(\mathrm{x})) \geq -\alpha(h_i(\mathrm{x})) \Big\} \tag{6}$$

where $\alpha(\cdot)$ is a class-$\mathcal{K}_\infty$ function.

Instead of considering control inputs directly, the notion of a control barrier corridor allows us to focus on feedback control goal states to investigate how CBFs encode safety geometrically. A natural question is whether, and under what conditions, the goal states in $\mathrm{BC}(\mathrm{x})$ partially or fully share the safety properties of the state x. It is also important to observe that $\mathrm{BC}(\mathrm{x})$ can, in general, have an arbitrarily complex shape and topological connectivity, depending on the properties of the CBFs $h_i(\mathrm{x})$, the system dynamics $f(\mathrm{x},\mathrm{u})$, and the goal control policy $k_{\mathrm{x}^*}(\mathrm{x})$. Hence, next we study examples of control barrier corridors for widely used system models and investigate the impact of CBF convexity:

$$h_i(\mathrm{x}^*) \geq h_i(\mathrm{x}) + \nabla h_i(\mathrm{x})(\mathrm{x}^* - \mathrm{x}).$$

III. Examples of Control Barrier Corridors

In this section, we present example constructions of control barrier corridors for fully actuated systems with proportional control, unicycle systems with inner-outer loop control, and linear systems with output regulation control.

A. Control Barrier Corridors of Fully Actuated Systems

As the first example, assuming full-state feedback linearization of control systems, we consider a simple yet nontrivial and informative case: the first-order fully actuated kinematic system model with proportional feedback control,

$$\dot{\mathrm{x}} = \mathrm{u}, \quad \text{and} \quad \mathrm{u} = -\kappa(\mathrm{x}-\mathrm{x}^*), \tag{7}$$

where $\kappa > 0$ is a fixed control gain determining the exponential convergence rate of the closed-loop system to any given goal state $\mathrm{x}^* \in \mathbb{R}^{n_\mathrm{x}}$. For simplicity, we also consider a linear barrier decay rate function $\alpha(x) = \alpha x$, which corresponds to an exponential decay rate for the lower bound of the barrier function value. Accordingly, for a given set of control barrier functions $h_1(\mathrm{x}), \ldots, h_m(\mathrm{x})$ of the fully actuated system $\dot{\mathrm{x}} = \mathrm{u}$, under proportional goal control $\mathrm{u} = -\kappa(\mathrm{x}-\mathrm{x}^*)$, the control barrier corridor $\mathrm{BC}_{\mathrm{full}}(\mathrm{x})$ around a safe robot state $\mathrm{x} \in \mathbb{R}^{n_\mathrm{x}}$ (with $h_i(\mathrm{x}) \geq 0$ for all i) contains all possible goal states $\mathrm{x}^* \in \mathbb{R}^{n_\mathrm{x}}$ that ensure safety feasibility and is given by

$$\mathrm{BC}_{\mathrm{full}}(\mathrm{x}) = \bigcap_{i=1}^{m} \Big\{ \mathrm{x}^* \in \mathbb{R}^{n_\mathrm{x}} \Big| -\kappa \nabla h_i(\mathrm{x})^{\mathrm{T}}(\mathrm{x}-\mathrm{x}^*) \geq -\alpha h_i(\mathrm{x}) \Big\} \tag{8}$$

where $\kappa > 0$ is the proportional control gain and $\alpha > 0$ is the linear barrier decay rate. Note that the control barrier corridor $\mathrm{BC}_{\mathrm{full}}(\mathrm{x})$ is a convex intersection of halfspaces and contains the safe robot state $\mathrm{x} \in \mathrm{BC}_{\mathrm{full}}(\mathrm{x})$. Moreover, its convex shape depends on the control barrier functions and the ratio of the control gain κ and the barrier rate α. An important question is: how do the control barrier functions influence the barrier corridor, and what are the potential consequences of (mis)matching the control convergence rate with the barrier decay rate? We observe that a higher barrier decay rate increases system confidence, aggressiveness, and risk-taking, whereas a higher control convergence rate leads to caution, conservativeness, and risk avoidance, see Fig. 2. We show below that, in order to extend robot safety locally within the control barrier corridor, the convergence rate of the control and the allowed decay rate of barrier safety need to match (revealing a trade-off between safety and reactiveness) and the control barrier functions needs to be convex.

Proposition 1 (The Geometry of Safety Meets the Dynamics of Safety) *If the control barrier functions $h_1(\mathrm{x}), \ldots, h_m(\mathrm{x})$ are convex and the proportional control gain κ and the*

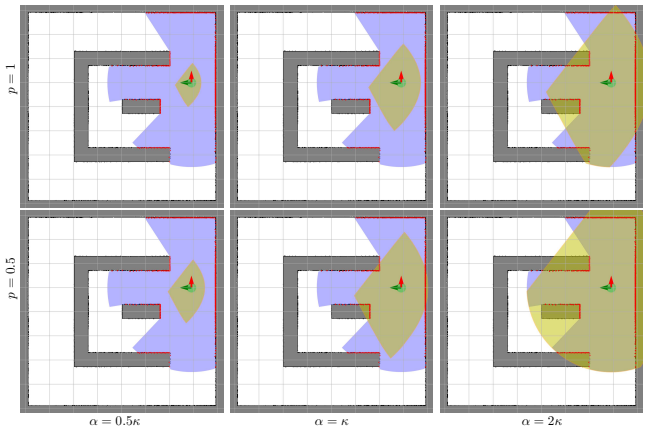

Fig. 2. The influence of the proportional control gain κ, barrier decay rate α, and the order p of the power distance on control barrier corridors (yellow) of a fully actuated robot (cyan) relative to sensed obstacle points (red). A control barrier corridor corresponds to a local safe zone around the robot (cyan), free of obstacles (red), for a pair of matching barrier rate and control gain ($\alpha = \kappa$), and convex barrier functions ($p \geq 1$). The conservativeness of the barrier corridor increases with higher control gain ($\alpha < \kappa$) and higher barrier convexity ($p > 1$), and it becomes less accurate with increasing barrier rate ($\alpha > \kappa$) and increasing barrier concavity ($p < 1$).

barrier decay rate α are the same (i.e., $\alpha = \kappa$), then any goal state $\mathrm{x}^* \in \mathrm{BC}_{\mathrm{full}}(\mathrm{x})$ in the convex control barrier corridor

$$\mathrm{BC}_{\mathrm{full}}(\mathrm{x}) = \bigcap_{i=1}^{m} \left\{ \mathrm{x}^* \in \mathbb{R}^{n_{\mathrm{x}}} \middle| h_i(\mathrm{x}) + \nabla h_i(\mathrm{x})^{\mathrm{T}}(\mathrm{x}^* - \mathrm{x}) \geq 0 \right\}$$

of a safe state x (i.e., $h_i(\mathrm{x}) \geq 0$ for all i) is also safe, due to the first-order condition of convexity, i.e.,

$$h_i(\mathrm{x}^*) \geq h_i(\mathrm{x}) + \nabla h_i(\mathrm{x})^{\mathrm{T}}(\mathrm{x}^* - \mathrm{x}) \geq 0, \tag{9}$$

which makes $\mathrm{BC}_{\mathrm{full}}(\mathrm{x})$ a local safe neighborhood around x.

Proof. The result directly follows from the first-order condition of convexity for $\alpha = \kappa$. ■

Another practical question is: Once a goal in the control barrier corridor is selected, how to ensure that the goal remains safely reachable for all future times for persistent goal control. Inspired by higher-order control barrier functions [33], we define the goal-control barrier function $h_{i,\mathrm{x}^*}(\mathrm{x})$ as

$$h_{i,\mathrm{x}^*}(\mathrm{x}) = -\kappa \nabla h_i(\mathrm{x})^{\mathrm{T}}(\mathrm{x} - \mathrm{x}^*) + \alpha h_i(\mathrm{x}) \tag{10}$$

which results in the following safe control constraint for goal safety for the fully actuated kinematic system $\dot{\mathrm{x}} = \mathrm{u}$:

$$\dot{h}_{i,\mathrm{x}^*}(\mathrm{x}) = \nabla h_{i,\mathrm{x}^*}(\mathrm{x})^{\mathrm{T}}\mathrm{u} \geq -\alpha h_{i,\mathrm{x}^*}(\mathrm{x}) \tag{11}$$

where the gradient of the goal-control barrier function $h_{i,\mathrm{x}^*}(\mathrm{x})$ is given in terms of the Hessian $\nabla^2 h_i(\mathrm{x})$ and gradient $\nabla h_i(\mathrm{x})$ of the control barrier function $h_i(\mathrm{x})$ as

$$\nabla h_{i,\mathrm{x}^*}(\mathrm{x}) = -\kappa \nabla^2 h_i(\mathrm{x})(\mathrm{x} - \mathrm{x}^*) + (\alpha - \kappa)\nabla h_i(\mathrm{x}). \tag{12}$$

The safety feasibility of goal-control barrier functions under proportional control ensures that the same goal can be persistently selected from a continuously evolving barrier corridor.

Proposition 2 (Safe and Persistent Goal Control) *For any convex control barrier functions $h_1(\mathrm{x}), \ldots, h_m(\mathrm{x})$, and any matching pair $\alpha = \kappa$ of the control gain and the barrier rate, the fully actuated system $\dot{\mathrm{x}} = \mathrm{u}$ under the proportional goal control $\mathrm{u} = -\kappa(\mathrm{x} - \mathrm{x}^*)$ asymptotically and safely brings any initial safe state $\mathrm{x}(0) \in \mathbb{R}^{n_{\mathrm{x}}}$ (with $h_i(\mathrm{x}(0)) \geq 0$ for all i) to any safe goal $\mathrm{x}^* \in \mathrm{BC}_{\mathrm{full}}(\mathrm{x}(0))$, while ensuring that the goal x^* remains in the barrier corridor $\mathrm{BC}_{\mathrm{full}}(\mathrm{x}(t))$ along the closed-loop trajectory $\mathrm{x}(t)$ for all future times $t \geq 0$, i.e.,*

$$\begin{aligned} &h_i(\mathrm{x}(t)) \geq 0 \quad \forall t \geq 0, i = 1, \ldots, m, \\ &\mathrm{x}^* \in \mathrm{BC}_{\mathrm{full}}(\mathrm{x}(t)) \quad \forall t \geq 0, \\ &\lim_{t \to \infty} \mathrm{x}(t) = \mathrm{x}^*. \end{aligned}$$

Proof. Starting at $t = 0$ from $\mathrm{x}(0) = \mathrm{x}_0$, the closed-loop trajectory of $\dot{\mathrm{x}} = -\kappa(\mathrm{x} - \mathrm{x}^*)$ is given by

$$\mathrm{x}(t) = e^{-\kappa t}\mathrm{x}_0 + (1 - e^{-\kappa t})\mathrm{x}^*, \quad t \geq 0,$$

which converges exponentially to x^* and corresponds to the safe line segment $[\mathrm{x}_0, \mathrm{x}^*] \subseteq \mathrm{BC}_{\mathrm{full}}(\mathrm{x}_0)$ within the convex safe barrier corridor $\mathrm{BC}_{\mathrm{full}}(\mathrm{x}_0)$, see Proposition 1.

Moreover, since $\mathrm{x}^* \in \mathrm{BC}_{\mathrm{full}}(\mathrm{x}_0)$, we have $h_{i,\mathrm{x}^*}(\mathrm{x}_0) \geq 0$ at the start at $t = 0$. Hence, the persistent inclusion of the goal in the barrier corridor (i.e., $\mathrm{x}^* \in \mathrm{BC}_{\mathrm{full}}(\mathrm{x}(t))$) follows from the fact that the safety feasibility of the goal-control barrier function is ensured under proportional control, i.e.,

$$\begin{aligned} \dot{h}_{i,\mathrm{x}^*}(\mathrm{x}) &= -\kappa \nabla h_{i,\mathrm{x}^*}(\mathrm{x})^{\mathrm{T}}(\mathrm{x} - \mathrm{x}^*) = \kappa^2 (\mathrm{x} - \mathrm{x}^*)^{\mathrm{T}} \nabla^2 h(\mathrm{x})(\mathrm{x} - \mathrm{x}^*) \\ &\geq 0 \geq -\alpha h_{i,\mathrm{x}^*}(\mathrm{x}), \end{aligned}$$

since $\nabla h_{i,\mathrm{x}^*}(\mathrm{x}) = -\kappa \nabla^2 h_i(\mathrm{x})(\mathrm{x} - \mathrm{x}^*)$ for $\alpha = \kappa$, and the Hessian of a convex function is positive definite. ■

B. Control Barrier Corridors of Kinematic Unicycle Systems

Control-affine systems of the form $\dot{\mathrm{x}} = f(\mathrm{x}) + g(\mathrm{x})\mathrm{u}$ allow for a convex quadratic optimization formulation of safety filtering of control inputs as in (2). However, the general nonlinear transformation of the control input (i.e., $g(\mathrm{x})\mathrm{u}$) makes it difficult to fully understand, in geometric terms, the local influence of control on state safety. In this part, as an example of control-affine systems, we present a construction of control barrier corridors for kinematic unicycle systems under a standard geometric feedback control policy for goal-point navigation. In particular, we consider a kinematic unicycle robot, with position $\mathrm{x} \in \mathbb{R}^2$ and forward orientation $\theta \in [-\pi, \pi)$, whose equations of motion are given by

$$\dot{\mathrm{x}} = v \begin{bmatrix} \cos\theta \\ \sin\theta \end{bmatrix}, \quad \text{and} \quad \dot{\theta} = \omega, \tag{13}$$

where $v \in \mathbb{R}$ and $\omega \in \mathbb{R}$ are the scalar control inputs specifying the linear and angular velocities, respectively.

Using a standard inner-outer loop control architecture [20], [35], the unicycle dynamics can be globally asymptotically brought to any goal position $\mathrm{x}^* \in \mathbb{R}^2$ by minimizing the distance to the goal (outer loop) and the angular alignment error (inner loop), with the control inputs given by

$$v = -\kappa_v \begin{bmatrix} \cos\theta \\ \sin\theta \end{bmatrix}^{\mathrm{T}} (\mathrm{x} - \mathrm{x}^*), \tag{14a}$$

$$\omega = \kappa_\omega \operatorname{atan2}\left(\begin{bmatrix} -\sin\theta \\ \cos\theta \end{bmatrix}^{\mathrm{T}} (\mathrm{x}^* - \mathrm{x}), \begin{bmatrix} \cos\theta \\ \sin\theta \end{bmatrix}^{\mathrm{T}} (\mathrm{x}^* - \mathrm{x}) \right) \tag{14b}$$

where $\operatorname{atan2}(y, x)$ is the two-argument arctangent function.

A practical feature of circular unicycle robots (e.g., cleaning robots) is that they can freely perform turns in place

with no collision with obstacles. Accordingly, for a given set of control barrier functions $h_1(\mathrm{x}), \ldots, h_m(\mathrm{x})$ assessing the safety of the unicycle position x irrespective of its orientation θ (e.g., power distance to collision), we determine the control barrier corridor of the closed-loop unicycle system as the set of goal positions that yields safe control as

$$\mathrm{BC}_{\mathrm{uni}}(\mathrm{x},\theta) = \bigcap_{i=1}^{m} \left\{ \mathrm{x}^* \in \mathbb{R}^2 \,\middle|\, -\kappa_v \nabla h_i(\mathrm{x})^{\mathrm{T}} \begin{bmatrix} \cos\theta \\ \sin\theta \end{bmatrix} \begin{bmatrix} \cos\theta \\ \sin\theta \end{bmatrix}^{\mathrm{T}} (\mathrm{x}-\mathrm{x}^*) \geq -\alpha h_i(\mathrm{x}) \right\}$$
$$= \bigcap_{i=1}^{m} \left\{ \mathrm{x}^* \in \mathbb{R}^2 \,\middle|\, -\kappa_v \nabla h_i(\mathrm{x})^{\mathrm{T}} \left(\mathbf{I} - \begin{bmatrix} -\sin\theta \\ \cos\theta \end{bmatrix} \begin{bmatrix} -\sin\theta \\ \cos\theta \end{bmatrix}^{\mathrm{T}} \right) (\mathrm{x}-\mathrm{x}^*) \geq -\alpha h_i(\mathrm{x}) \right\} \quad (15)$$

where $\alpha > 0$ is a constant barrier decay rate. Note that the unicycle control barrier corridor $\mathrm{BC}_{\mathrm{uni}}(\mathrm{x},\theta)$ in (15) is larger than, and contains, the fully actuated control barrier corridor $\mathrm{BC}_{\mathrm{full}}(\mathrm{x})$ in (8) (for the same control gains $\kappa_v = \kappa$), i.e., $\mathrm{BC}_{\mathrm{full}}(\mathrm{x}) \subset \mathrm{BC}_{\mathrm{uni}}(\mathrm{x},\theta)$, but it does not define a local safe neighborhood of a unicycle pose, because the nonholonomic motion constraint inherently ensures lateral safety in the sideways direction. On the other hand, ensuring safety in all directions results in the full control barrier corridor, i.e.,

$$\mathrm{BC}_{\mathrm{full}}(\mathrm{x}) = \bigcap_{-\pi \leq \theta \leq \pi} \mathrm{BC}_{\mathrm{uni}}(\mathrm{x},\theta), \quad (16)$$

which makes the full control barrier corridor a local safe zone candidate for goal selection in unicycle control.

Another known technical challenge of unicycle dynamics is that the nonholonomic motion constraint does not permit continuous smooth control toward a goal position x^* at the critical barrier safety boundary, where $h_i(\mathrm{x}^*) = 0$ for some i, and therefore requires an open safe neighborhood around the goal location to reach it with continuous and smooth control [20]. Hence, given any desired extra safety margin $\varepsilon \geq 0$, we define an ε-safer full control barrier corridor of a safe state x, with $h_i(\mathrm{x}) \geq 0$ for all i, as

$$\mathrm{BC}_{\mathrm{full},\varepsilon}(\mathrm{x}) = \bigcap_{i=1}^{m} \left\{ \mathrm{x}^* \in \mathbb{R}^2 \,\middle|\, -\kappa \nabla h_{i,\varepsilon}(\mathrm{x})^{\mathrm{T}} (\mathrm{x}-\mathrm{x}^*) \geq -\alpha h_{i,\varepsilon}(\mathrm{x}) \right\}$$
$$= \bigcap_{i=1}^{m} \left\{ \mathrm{x}^* \in \mathbb{R}^2 \,\middle|\, -\kappa \nabla h_i(\mathrm{x})^{\mathrm{T}} (\mathrm{x}-\mathrm{x}^*) \geq -\alpha (h_i(\mathrm{x}) - \varepsilon) \right\} \quad (17)$$

based on the ε-safer control barrier functions defined to be

$$h_{i,\varepsilon}(\mathrm{x}) = h_i(\mathrm{x}) - \varepsilon, \quad (18)$$

where $\nabla h_{i,\varepsilon}(\mathrm{x}) = \nabla h_i(\mathrm{x})$. For persistent selection of an ε-safer goal x^* in $\mathrm{BC}_{\mathrm{full},\varepsilon}(\mathrm{x})$, we also define the ε-safer goal-control barrier functions as

$$h_{i,\mathrm{x}^*,\varepsilon}(\mathrm{x}) = -\kappa \nabla h_i(\mathrm{x})^{\mathrm{T}} (\mathrm{x} - \mathrm{x}^*) + \alpha (h_i(\mathrm{x}) - \varepsilon) \quad (19)$$

whose gradient is given by

$$\nabla h_{i,\mathrm{x}^*,\varepsilon}(\mathrm{x}) = -\kappa \nabla^2 h_i(\mathrm{x})(\mathrm{x} - \mathrm{x}^*) + (\alpha - \kappa) \nabla h_i(\mathrm{x}). \quad (20)$$

Accordingly, using control barrier functions $h_i(\mathrm{x})$ and the ε-safer goal-control barrier functions $h_{i,\mathrm{x}^*,\varepsilon}(\mathrm{x})$, we construct a safety filter for the reference linear velocity in (14a) of the unicycle dynamics in (13) to determine the safe linear velocity input that ensures both the safety of the robot and the persistent selection of an ε-safe goal $\mathrm{x}^* \in \mathrm{BC}_{\mathrm{full},\varepsilon}(\mathrm{x})$ as

$$\begin{aligned} \text{minimize} \quad & \left(v + \kappa \begin{bmatrix} \cos\theta \\ \sin\theta \end{bmatrix}^{\mathrm{T}} (\mathrm{x} - \mathrm{x}^*) \right)^2 \\ \text{subject to} \quad & \nabla h_i(\mathrm{x})^{\mathrm{T}} \begin{bmatrix} \cos\theta \\ \sin\theta \end{bmatrix} v \geq -\alpha h_i(\mathrm{x}) \quad \forall i \\ & \nabla h_{i,\mathrm{x}^*,\varepsilon}(\mathrm{x})^{\mathrm{T}} \begin{bmatrix} \cos\theta \\ \sin\theta \end{bmatrix} v \geq -\alpha h_{i,\mathrm{x}^*,\varepsilon}(\mathrm{x}) \quad \forall i \end{aligned} \quad (21)$$

and we determine the angular velocity input as in (14b). Note that the safe unicycle velocity control optimization in (21) is always feasible for any safe robot position x and ε-safer goal x^* in $\mathrm{BC}_{\mathrm{full},\varepsilon}(\mathrm{x})$ (since $v = 0$ is always safe for both the robot and persistent goal selection), and can be explicitly solved due to the one-dimensional optimization form.

Proposition 3 (Safe and Persistent Unicycle Goal Control) *Given any convex control barrier functions $h_i(\mathrm{x})$, a matching pair $\alpha = \kappa$ of control gain and barrier rate, and any positive safety margin $\varepsilon > 0$, the safe unicycle control in (21) and (14b) asymptotically and safely brings any safe unicycle pose (x,θ) (with $h_i(\mathrm{x}) \geq 0$ for all i) to any ε-safer goal $\mathrm{x}^* \in \mathrm{BC}_{\mathrm{full},\varepsilon}(\mathrm{x})$, while ensuring that the goal x^* remains in the ε-safer barrier corridor $\mathrm{BC}_{\mathrm{full},\varepsilon}(\mathrm{x}(t))$ along the closed-loop unicycle motion trajectory $(\mathrm{x}(t),\theta(t))$ for all $t \geq 0$, i.e.,*

$$\begin{aligned} & h_i(\mathrm{x}(t)) \geq 0 \quad \forall t \geq 0, i = 1, \ldots, m \\ & \mathrm{x}^* \in \mathrm{BC}_{\varepsilon}(\mathrm{x}(t)) \quad \forall t \geq 0, \\ & \lim_{t \to \infty} \mathrm{x}(t) = \mathrm{x}^*. \end{aligned}$$

Proof. If $\mathrm{BC}_{\mathrm{full},\varepsilon}(\mathrm{x}) = \varnothing$, then the statement holds trivially. Otherwise, the result can be verified as follows.

For convex barrier functions $h_i(\mathrm{x})$ and a matching control gain and barrier rate $\alpha = \kappa$, the full control barrier corridor $\mathrm{BC}_{\mathrm{full}}(\mathrm{x})$ in (8) is a local safe convex neighborhood of a safe unicycle position x (see Proposition 1). Moreover, by definition (17), the ε-safer full control barrier corridor $\mathrm{BC}_{\mathrm{full},\varepsilon}(\mathrm{x})$ is a convex subset of $\mathrm{BC}_{\mathrm{full}}(\mathrm{x})$. Therefore, the straight line between the robot position x and the goal position x^* is safe and contained in $\mathrm{BC}_{\mathrm{full}}(\mathrm{x})$, i.e.,

$$\mathrm{x}^* \in \mathrm{BC}_{\mathrm{full},\varepsilon}(\mathrm{x}) \subset \mathrm{BC}_{\mathrm{full}}(\mathrm{x}), \text{ and } [\mathrm{x}^*, \mathrm{x}] \subseteq \mathrm{BC}_{\mathrm{full}}(\mathrm{x}).$$

The optimal safe velocity control always exists (since $v = 0$ is feasible) and, by design, it ensures the safety of the robot position x and the persistent selection of the goal x^*. Moreover, it satisfies $-\kappa \begin{bmatrix} \cos\theta \\ \sin\theta \end{bmatrix}^{\mathrm{T}} (\mathrm{x} - \mathrm{x}^*) v \geq 0$ and so the distance to the goal decreases over time as

$$\frac{\mathrm{d}}{\mathrm{d}t} \|\mathrm{x} - \mathrm{x}^*\|^2 = \begin{bmatrix} \cos\theta \\ \sin\theta \end{bmatrix}^{\mathrm{T}} (\mathrm{x} - \mathrm{x}^*) v \leq 0$$

which can be zero only when $v = 0$. If $v = 0$, the angular velocity control in (14b) exponentially aligns the robot's orientation with the goal x^*. Since the goal remains ε-safer in $\mathrm{BC}_{\mathrm{full},\varepsilon}(\mathrm{x}) \subset \mathrm{BC}_{\mathrm{full}}(\mathrm{x})$ for all times, the linear velocity v is guaranteed to become positive after a finite time and so the robot continuously move toward the goal. ■

C. Control Barrier Corridors of Linear Control Systems

As a third example of control barrier corridors, we consider a linear time-invariant system:

$$\dot{\mathrm{x}} = A\mathrm{x} + B\mathrm{u}, \quad \mathrm{y} = C\mathrm{x}, \quad (22)$$

where $\mathrm{x} \in \mathbb{R}^{n_{\mathrm{x}}}$ is the state (e.g., position and velocity), $\mathrm{u} \in \mathbb{R}^{n_{\mathrm{u}}}$ is the control input (e.g., acceleration), and $\mathrm{y} \in \mathbb{R}^{n_{\mathrm{y}}}$ is the output (e.g., position). A, B, C are, respectively, the state, input, and output matrices of appropriate dimensions.

We assume that the pair (A, B) is stabilizable and $K \in \mathbb{R}^{n_u \times n_x}$ is a feedback matrix such that $A+BK$ is Hurwitz. We also assume that $\begin{bmatrix} A & B \\ C & 0 \end{bmatrix}$ is invertible, so that the output can be related to the state and control via the output-to-state and output-to-control matrices, X and U, given by

$$\begin{bmatrix} X \\ U \end{bmatrix} = \begin{bmatrix} A & B \\ C & 0 \end{bmatrix}^{-1} \begin{bmatrix} 0 \\ I \end{bmatrix}. \tag{23}$$

This ensures that the output-to-state-to-output mapping is the identity, i.e., $CX = I$ and $\mathrm{y} = CX\mathrm{y}$ for all y, and that output regulation vanishes at steady state, i.e., $AX + BU = 0$ and $AX\mathrm{y} + BU\mathrm{y} = 0$ for all y. Hence, given any desired output y^*, the state-feedback output regulation control policy [36]:

$$u = k_{\mathrm{y}^*}(\mathrm{x}) = K(\mathrm{x} - X\mathrm{y}^*) + U\mathrm{y}^* \tag{24}$$

renders $\mathrm{x}^* = X\mathrm{y}^*$ an exponentially stable equilibrium of the closed-loop system dynamics:

$$\dot{\mathrm{x}} = (A + BK)(\mathrm{x} - X\mathrm{y}^*), \quad \mathrm{y} = C\mathrm{x}, \tag{25}$$

and ensures that the output y converges exponentially to y^*.

Given a set of control barrier functions $h_1(\mathrm{x}), \dots, h_m(\mathrm{x})$, the control barrier corridor of the linear control system in (22), under the output regulation control in (24), contains all desired system outputs y^* that ensure safety feasibility at a safe system state x with $h_i(\mathrm{x}) \geq 0$ as

$$\mathrm{BC}_{\mathrm{lor}}(\mathrm{x}) = \bigcap_{i=1}^{m} \left\{ \mathrm{y}^* \middle| \nabla h_i(\mathrm{x})^{\mathrm{T}}(A+BK)(\mathrm{x}-X\mathrm{y}^*) \geq -\alpha(h_i(\mathrm{x})) \right\} \tag{26}$$

which is convex, being the intersection of halfspaces. Note that, in general, the control barrier corridor $\mathrm{BC}_{\mathrm{lor}}(\mathrm{x})$ of the linear output regulator system can be empty, especially for high-order systems, and that the current system output $\mathrm{y} = C\mathrm{x}$ is not necessarily in the barrier corridor $\mathrm{BC}_{\mathrm{lor}}(\mathrm{x})$. Hence, persistent desired output selection and regulation (as in Proposition 2) is not guaranteed in general. A promising open research question is how to design a control policy and determine requirements on control barrier functions for linear output regulation systems such that for any safe state x:

- (Recursive Feasibility) the control barrier corridor is nonempty, i.e., $\mathrm{BC}_{\mathrm{lor}}(\mathrm{x}) \neq \varnothing$;
- (Local Neighborhood) the control barrier corridor contains the current output, i.e., $\mathrm{y} = C\mathrm{x} \in \mathrm{BC}_{\mathrm{lor}}(\mathrm{x})$;
- (Persistent Output Regulation) the control barrier corridor ensures persistent and safe output regulation, i.e., $h_i(\mathrm{x}(t)) \geq 0$ and $\mathrm{y}^* \in \mathrm{BC}(\mathrm{x}(t))$ for all $t \geq 0$, given that $h_i(\mathrm{x}(0)) \geq 0$ and $\mathrm{y}^* \in \mathrm{BC}(\mathrm{x}(0))$.

For example, if both B and C are invertible, all these desired features can be satisfied via full state-feedback linearization by embedding the fully-actuated reference system dynamics $\dot{\mathrm{x}} = -\kappa(\mathrm{x} - \mathrm{x}^*)$, where $\mathrm{x}^* = C^{-1}y^*$, by setting $X = C^{-1}$, $U = -B^{-1}AC^{-1}$, and $K = -B^{-1}(\kappa I + A)$.

In the general case, similar to the goal-control barrier functions in (10), to ensure the inclusion of the current output in the control barrier corridor and persistent desired output regulation, one may consider the current-output and goal-output control barrier functions, respectively, defined as

$$h_{i,\mathrm{y}}(\mathrm{x}) = \nabla h_i(\mathrm{x})^{\mathrm{T}}(A+BK)(I-XC)\mathrm{x} + \alpha(h_i(\mathrm{x})), \tag{27}$$

$$h_{i,\mathrm{y}^*}(\mathrm{x}) = \nabla h_i(\mathrm{x})^{\mathrm{T}}(A+BK)(\mathrm{x}-X\mathrm{y}^*) + \alpha(h_i(\mathrm{x})), \tag{28}$$

where $h_{i,\mathrm{y}}(\mathrm{x}) \geq 0$ implies $\mathrm{y} = C\mathrm{x} \in \mathrm{BC}_{\mathrm{lor}}(\mathrm{x})$, and $h_{i,\mathrm{y}^*}(\mathrm{x}) \geq 0$ implies $\mathrm{y}^* \in \mathrm{BC}_{\mathrm{lor}}(\mathrm{x})$. Thus, the safety feasibility of output-control barrier functions can be used as constraints for recursive feasibility and persistent regulation.

Finally, we consider the following trust region:

$$\mathrm{TR}(\mathrm{x}) = \bigcap_{i=1}^{m} \left\{ \mathrm{y}^* \middle| \|\nabla h_i(\mathrm{x})\| \|A+BK\| \|\mathrm{x}-X\mathrm{y}^*\| \leq \alpha(h_i(\mathrm{x})) \right\} \tag{29}$$

which satisfies $\mathrm{TR}(\mathrm{x}) \subseteq \mathrm{BC}_{\mathrm{lor}}(\mathrm{x})$, by the Cauchy–Schwarz inequality, and offers a sufficient condition for persistency.

Proposition 4 (Safe and Persistent Output Regulation) *Consider the closed-loop system in* (25) *and the set* $\mathrm{TR}(\mathrm{x}) \subseteq \mathrm{BC}_{\mathrm{lor}}(\mathrm{x})$ *in* (29)*. If the control barrier functions* $h_i(\mathrm{x})$ *are convex and the barrier decay function* $\alpha(.)$ *satisfies*

$$\alpha(h_i(\mathrm{x})) \leq \tfrac{1}{2}\|A + BK\| h_i(\mathrm{x}), \tag{30}$$

then any desired output $\mathrm{y}^* \in \mathrm{TR}(\mathrm{x})$ *is safely reachable, i.e.,* $h_i(\mathrm{x}(t)) \geq 0$ *along the closed-loop trajectory* $\mathrm{x}(t)$ *for all* $t \geq 0$.

Proof. Let $L := A + BK$, $\mathrm{z} := X\mathrm{y}^* - \mathrm{x}$, and $g_i := \nabla h_i(\mathrm{x})$ to simplify the notation. Since $\mathrm{y}^* \in \mathrm{TR}(\mathrm{x})$ by assumption and by the Cauchy–Schwarz inequality

$$0 \leq \alpha(h_i(\mathrm{x})) - \|L\|\|g_i\|\|\mathrm{z}\| \leq \alpha(h_i(\mathrm{x})) + \|L\| g_i^{\top}\mathrm{z}. \tag{31}$$

To relate (31) to $\mathrm{x}(t) = e^{Lt}\mathrm{x} + (I - e^{Lt})X\mathrm{y}^*$ starting from x at $t = 0$, we add and subtract $\|L\| g_i^{\top} e^{Lt}\mathrm{z}$, which satisfies $\|L\| g_i^{\top} e^{Lt}\mathrm{z} \leq \|L\|\|g_i\|\|e^{Lt}\|\|\mathrm{z}\| \leq \|L\|\|g_i\|\|\mathrm{z}\| \leq \alpha(h_i(\mathrm{x}))$ by the Cauchy–Schwarz inequality, $\|e^{Lt}\| \leq 1$ for all t, and (29). Thus, we verify that $h_i(\mathrm{x}(t)) \geq 0$ as follows:

$$\begin{aligned} 0 &\leq \alpha(h_i(\mathrm{x})) + \|L\| g_i^{\top}\mathrm{z} - \|L\| g_i^{\top} e^{Lt}\mathrm{z} + \|L\| g_i^{\top} e^{Lt}\mathrm{z} \\ &\leq \alpha(h_i(\mathrm{x})) + \|L\| g_i^{\top}(I - e^{Lt})\mathrm{z} + \|L\|\|g_i\|\|\mathrm{z}\| \\ &\leq 2\alpha(h_i(\mathrm{x})) + \|L\| g_i^{\top}(\mathrm{x}(t) - \mathrm{x}) \\ &\leq \|L\|(h_i(\mathrm{x}) + g_i^{\top}(\mathrm{x}(t) - \mathrm{x})) \leq \|L\| h_i(\mathrm{x}(t)), \end{aligned}$$

where we use the choice of α in (30) in the second-to-last step and the convexity of h_i in the last step. ■

IV. Application of Control Barrier Corridors: Safe and Persistent Path Following

In this section, we present an application of control barrier corridors for goal selection in safe and persistent path following and demonstrate sensor-based control for mobile robot exploration in unknown environments.

A. Safe Path Following with Control Barrier Corridors

A practical use of control barrier corridors is local goal selection for safe and persistent path following around obstacles, ensuring collision avoidance while maintaining continuous progress along a path. Given a reference path $\mathrm{p}(s) : [0, 1] \to \mathbb{R}^n$, starting at $\mathrm{p}(0)$ and ending at $\mathrm{p}(1)$, we consider local path goal selection using the control barrier corridor $\mathrm{BC}(\mathrm{x})$ of a closed-loop robot system. Let x be a safe robot state (with $h_i(\mathrm{x}) \geq i$ for all i). We select the farthest path point $\mathrm{p}(s)$ contained within $\mathrm{BC}(\mathrm{x})$:

$$\mathrm{p}^*(\mathrm{x}) := \mathrm{p}\begin{pmatrix} \arg\max\limits_{\substack{s \in [0,1] \\ \mathrm{p}(s) \in \mathrm{BC}(\mathrm{x})}} s \end{pmatrix}. \tag{32}$$

The local safety of control barrier corridors plays a critical role in ensuring the safe reachability of a selected path goal, as shown in Fig. 3. A matching pair of safety barrier decay rate and proportional control gain, $\alpha = \kappa$, together with convexity of the CBFs (see Proposition 1), enables safe goal selection in control barrier corridors, thereby ensuring verifiable and reliable path following around obstacles.

Proposition 5 (Safe and Persistent Path Following) *Let $h_1(\mathrm{x}), \dots, h_m(\mathrm{x})$ be convex and $\mathrm{p} : [0,1] \to \mathbb{R}^n$ be a strictly safe reference path, i.e., $h_i(\mathrm{p}(s)) > 0$ for all $s \in [0,1]$ and $i = 1, \dots, m$. Consider a fully actuated system under proportional control towards the farthest path point $\mathrm{p}^*(\mathrm{x})$ in (32) in the barrier corridor $\mathrm{BC}_{\mathrm{full}}(\mathrm{x})$ in (8):*

$$\dot{\mathrm{x}} = -\kappa\big(\mathrm{x} - \mathrm{p}^*(\mathrm{x})\big). \tag{33}$$

If the barrier rate and control gain are matching, $\alpha = \kappa$, starting from any initial safe state x_0 with $\mathrm{p}([0,1]) \cap \mathrm{BC}_{\mathrm{full}}(\mathrm{x}_0) \neq \varnothing$, the trajectory $\mathrm{x}(t)$ of the closed-loop system in (33) remains safe, has a safely reachable path goal at all times, persistently makes progress along the path $\mathrm{p}(s)$, and converges asymptotically to the end of the path $\mathrm{p}^*(1)$, i.e.,

$$\begin{aligned} h(\mathrm{x}(t)) &\geq 0, \quad \forall\, t \geq 0, \\ \mathrm{p}([0,1]) \cap \mathrm{BC}(\mathrm{x}(t)) &\neq \varnothing, \quad \forall\, t \geq 0, \\ \underset{\substack{s\in[0,1] \\ \mathrm{p}(s)\in\mathrm{BC}(\mathrm{x}(t_1))}}{\arg\max}\ s \ &\leq \underset{\substack{s\in[0,1] \\ \mathrm{p}(s)\in\mathrm{BC}(\mathrm{x}(t_2))}}{\arg\max}\ s, \quad \forall\, 0 \leq t_1 \leq t_2, \\ \lim_{t\to\infty} \mathrm{x}(t) &= \mathrm{p}(1). \end{aligned}$$

Proof. The safety of the trajectory $\mathrm{x}(t)$ follows from the definition in (8), which states that any goal $\mathrm{x}^* \in \mathrm{BC}_{\mathrm{full}}(\mathrm{x}(t))$ ensures safety feasibility under the proportional goal control $\mathrm{u} = -\kappa(\mathrm{x} - \mathrm{x}^*)$. The existence of a safely reachable path goal at all times is a consequence of the safe and persistent goal property of the full control barrier corridor $\mathrm{BC}_{\mathrm{full}}(\mathrm{x})$ in Proposition 1 and Proposition 2. The persistent goal property in Proposition 2 also ensures persistent progress along the reference path, since the previously selected goal is instantaneously maintained within $\mathrm{BC}_{\mathrm{full}}(\mathrm{x})$, while the farthest-path goal selection in (32) may either keep it or replace it with a farther point if available. Finally, since all path points are strictly safe (i.e., $h_i(\mathrm{p}(s)) > 0$), the control barrier corridor around any path point $\mathrm{BC}_{\mathrm{full}}(\mathrm{p}(s))$ has a nonempty interior with nonzero measure, ensuring that the robot can remain at a path point only for a finite time, except when asymptotically converging to the endpoint $\mathrm{p}(1)$. ■

Note that a similar conclusion also holds for the persistent unicycle control in Proposition 3 for ε-safer reference paths.

B. Sensor-Based Path Following for Mobile Exploration

We consider frontier-based autonomous robot exploration of unknown environments [37] to demonstrate the applicability of control barrier corridors to sensor-based safe navigation. We use a mobile robot in the Gazebo simulator with unicycle dynamics, known state, and a 2D laser scanner for obstacle sensing and occupancy mapping [38].

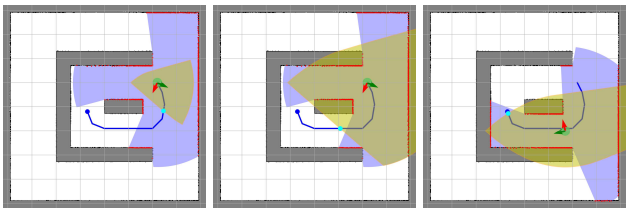

Fig. 3. Local goal selection (cyan) for following a reference path (blue) using a control barrier corridor (yellow). Matching the barrier decay rate and the control convergence rate ($\alpha = \kappa$, left) enables safe goal selection and reliable path-following control, as opposed to an unsafe and risky higher barrier decay rate than the control convergence rate ($\alpha = 3\kappa$, middle, right).

We construct control barrier corridors using the Euclidean distance (i.e., power distance with $p = 1$) to sensed obstacle points and impose a matching pair of linear velocity gain and barrier decay rate, $\alpha = \kappa_v$. The robot performs frontier-based exploration using the following sequential perception, planning, and control cycle:

i) Goal Frontier Selection: Choose a reachable frontier cell farthest from occupied cells (a simple measure of information utility), located between known-free and unknown regions of the current occupancy grid map.
ii) Safe Path Planning: Determine an optimal reference path (e.g., via graph search) using inverse distance to obstacles as local cost, minimizing path length while maximizing clearance.
iii) Safe Path Following: Select the farthest path point within the control barrier corridor as a local navigation goal, and navigate with persistent unicycle goal control (Proposition 3) until the path endpoint is reached or no longer reachable; otherwise, go to i).

Fig. 4 presents examples of selected frontiers, reference paths, local path goals, and control barrier corridors during autonomous exploration. The convex control barrier corridors are adaptively constructed and shaped as local collision-free zones around the robot using sensed obstacles and continuously evolve with the continuous robot motion. Once the farthest path point is selected as a safe goal for the unicycle, the unicycle control law not only ensures the robot safety but also maintains the goal within the barrier corridor for persistent progress along the exploration path (Proposition 3). Since safe and persistent path following only requires a safe reference path intersecting with the robot's control barrier corridor (Proposition 5), this enables replanning and updating the exploration path without coming to a stop.

V. Conclusions

This paper introduces control barrier corridors for closed-loop systems, transforming control barrier function constraints on the control inputs into geometric constraints on the reference goals of feedback control policies. Example control barrier constructions for fully actuated systems under proportional control, kinematic unicycle systems under inner-outer loop control, and linear systems under output regulation control show that individual state safety, encoded by control barrier functions, can be extended locally over control barrier corridors, enabling safe and persistent goal selection. We also demonstrate that constructing control barrier corridors

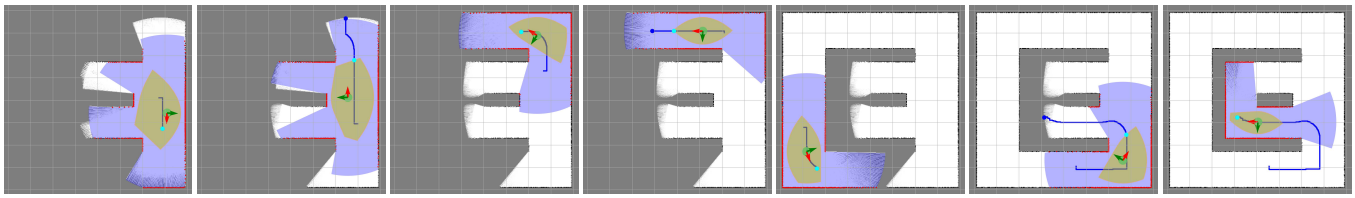

Fig. 4. Safe and persistent path following for frontier-based autonomous exploration of an unknown static environment, using a reference exploration path (blue line) toward a reachable frontier point (blue dot), with safely reachable path goal selection (cyan) over control barrier corridors (yellow) of a unicycle mobile robot (cyan + red arrow) constructed from sensed obstacle points (red) via an onboard laser scanner sensor.

directly from sensor observations enables verifiably safe, provably correct, and persistent autonomous robot navigation in unknown environments. Promising directions for future research include generalizations of control barrier corridors to higher-order systems using higher-order control barrier functions as well as leveraging control barrier corridors and control convergence rates to learn (neural) control barrier approximations with adaptive decay profiles.

REFERENCES

[1] A. D. Ames, S. Coogan, M. Egerstedt, G. Notomista, K. Sreenath, and P. Tabuada, "Control barrier functions: Theory and applications," in *European Control Conference*, 2019, pp. 3420–3431.

[2] R. Freeman and J. Primbs, "Control lyapunov functions: new ideas from an old source," in *IEEE Conference on Decision and Control*, vol. 4, 1996, pp. 3926–3931.

[3] M. Jankovic, "Combining control lyapunov and barrier functions for constrained stabilization of nonlinear systems," in *American Control Conference*, 2017, pp. 1916–1922.

[4] T. Marcucci, P. Nobel, R. Tedrake, and S. Boyd, "Fast path planning through large collections of safe boxes," *IEEE Transactions on Robotics*, vol. 40, pp. 3795–3811, 2024.

[5] S. Liu, M. Watterson, K. Mohta, K. Sun, S. Bhattacharya, C. J. Taylor, and V. Kumar, "Planning dynamically feasible trajectories for quadrotors using safe flight corridors in 3-d complex environments," *IEEE Robot. Autom. Lett.*, vol. 2, no. 3, pp. 1688–1695, 2017.

[6] I. Kolmanovsky, E. Garone, and S. D. Cairano, "Reference and command governors: A tutorial on their theory and automotive applications," in *American Control Conference*, 2014, pp. 226–241.

[7] O. Arslan and D. E. Koditschek, "Smooth extensions of feedback motion planners via reference governors," in *IEEE International Conference on Robotics and Automation*, 2017, pp. 4414–4421.

[8] K. Liang, M. Cai, and C.-I. Vasile, "Control barrier function for linearizable systems with high relative degrees from signal temporal logics: A reference governor approach," in *American Control Conference*, 2024, pp. 1676–1681.

[9] M. F. Reis, A. P. Aguiar, and P. Tabuada, "Control barrier function-based quadratic programs introduce undesirable asymptotically stable equilibria," *IEEE Control Syst. Lett.*, vol. 5, no. 2, pp. 731–736, 2021.

[10] Y. Yi, S. Koga, B. Gavrea, and N. Atanasov, "Control synthesis for stability and safety by differential complementarity problem," *IEEE Control Systems Letters*, vol. 7, pp. 895–900, 2023.

[11] X. Tan and D. V. Dimarogonas, "On the undesired equilibria induced by control barrier function based quadratic programs," *Automatica*, vol. 159, p. 111359, 2024.

[12] P. Braun and C. M. Kellett, "Comment on "stabilization with guaranteed safety using control lyapunov–barrier function"," *Automatica*, vol. 122, p. 109225, 2020.

[13] P. Mestres and J. Cortés, "Optimization-based safe stabilizing feedback with guaranteed region of attraction," *IEEE Control Systems Letters*, vol. 7, pp. 367–372, 2023.

[14] L. Wang, D. Han, and M. Egerstedt, "Permissive barrier certificates for safe stabilization using sum-of-squares," in *American Control Conference*, 2018, pp. 585–590.

[15] H. Dai, C. Jiang, H. Zhang, and A. Clark, "Verification and synthesis of compatible control lyapunov and control barrier functions," in *IEEE Conference on Decision and Control*, 2024, pp. 8178–8185.

[16] H. Parwana and D. Panagou, "Rate-tunable control barrier functions: Methods and algorithms for online adaptation," in *American Control Conference*, 2025, pp. 275–282.

[17] P. Ong, M. H. Cohen, T. G. Molnar, and A. D. Ames, "On the properties of optimal-decay control barrier functions," in *IEEE Conference on Decision and Control*, 2025.

[18] E. Garone and M. M. Nicotra, "Explicit reference governor for constrained nonlinear systems," *IEEE Transactions on Automatic Control*, vol. 61, no. 5, pp. 1379–1384, 2016.

[19] E. Gilbert and K. Tan, "Linear systems with state and control constraints: the theory and application of maximal output admissible sets," *IEEE Trans. Autom. Control*, vol. 36, no. 9, pp. 1008–1020, 1991.

[20] O. Arslan and D. E. Koditschek, "Sensor-based reactive navigation in unknown convex sphere worlds," *The International Journal of Robotics Research*, vol. 38, no. 2-3, pp. 196–223, 2019.

[21] A. İşleyen, N. van de Wouw, and Ö. Arslan, "Safe robot navigation using motion prediction and reference governor," *IEEE Robotics and Automation Letters*, vol. 7, no. 4, pp. 9715–9722, 2022.

[22] Z. Li, Ö. Arslan, and N. Atanasov, "Fast and safe path-following control using a state-dependent directional metric," in *IEEE International Conference on Robotics and Automation*, 2020, pp. 6176–6182.

[23] L. Burlion, R. Schieni, and I. V. Kolmanovsky, "A reference governor for linear systems with polynomial constraints," *Automatica*, vol. 142, p. 110313, 2022.

[24] Z. Li and N. Atanasov, "Governor-parameterized barrier function for safe output tracking with locally sensed constraints," *Automatica*, vol. 152, p. 110996, 2023.

[25] A. İşleyen, N. van de Wouw, and Ö. Arslan, "Feedback motion prediction for safe unicycle robot navigation," in *IEEE/RSJ Int. Conf. Intell. Robots Syst.*, 2023, pp. 10 511–10 518.

[26] A. İşleyen, N. Van De Wouw, and Ö. Arslan, "Adaptive headway motion control and motion prediction for safe unicycle motion design," in *IEEE Conference on Decision and Control*, 2023, pp. 6942–6949.

[27] G. Tartaglione, M. M. Nicotra, R. Naldi, and E. Garone, "A constrained control framework for unmanned aerial vehicles based on explicit reference governor," *Automatica*, vol. 166, p. 111696, 2024.

[28] K. Merckaert, B. Convens, M. M. Nicotra, and B. Vanderborght, "Real-time constraint-based planning and control of robotic manipulators for safe human–robot collaboration," *Robotics and Computer-Integrated Manufacturing*, vol. 87, p. 102711, 2024.

[29] R. Deits and R. Tedrake, "Computing large convex regions of obstacle-free space through semidefinite programming," in *Algorithmic Foundations of Robotics XI*, vol. 107, 2015, pp. 109–124.

[30] J. Chen, T. Liu, and S. Shen, "Online generation of collision-free trajectories for quadrotor flight in unknown cluttered environments," in *IEEE Int. Conf. Robot. Autom.*, 2016, pp. 1476–1483.

[31] D. Zhou, Z. Wang, S. Bandyopadhyay, and M. Schwager, "Fast, online collision avoidance for dynamic vehicles using buffered voronoi cells," *IEEE Robot. Autom. Lett.*, vol. 2, no. 2, pp. 1047–1054, 2017.

[32] Ö. Arslan and D. E. Koditschek, "Voronoi-based coverage control of heterogeneous disk-shaped robots," in *IEEE International Conference on Robotics and Automation*, 2016, pp. 4259–4266.

[33] W. Xiao and C. Belta, "High-order control barrier functions," *IEEE Trans. Autom. Control*, vol. 67, no. 7, pp. 3655–3662, 2022.

[34] A. D. Ames, X. Xu, J. W. Grizzle, and P. Tabuada, "Control barrier function based quadratic programs for safety critical systems," *IEEE Trans. Autom. Control*, vol. 62, no. 8, pp. 3861–3876, 2017.

[35] A. Astolfi, "Exponential stabilization of a wheeled mobile robot via discontinuous control," *Journal of dynamic systems, measurement, and control*, vol. 121, no. 1, pp. 121–126, 1999.

[36] J. Huang, *Nonlinear output regulation: theory and applications*. SIAM, 2004.

[37] B. Yamauchi, "A frontier-based approach for autonomous exploration," in *IEEE Int. Symp. Comput. Intell. Robot. Autom.*, 1997, pp. 146–151.

[38] A. Elfes, "Using occupancy grids for mobile robot perception and navigation," *Computer*, vol. 22, no. 6, pp. 46–57, 1989.